Transactions of the 15th International Conference on
Structural Mechanics in Reactor Technology (SMiRT-15)
Seoul, Korea, August 15-20, 1999

Assessment of Cracked Components Subjected to High Thermal Stress

Weilin Zang

SAQ Kontroll AB, Sweden

ABSTRACT

In the present study, a wide rang of two- and three-dimensional elastic-plastic *J*-integral calculations have been performed. The purpose of the analysis is to verify the accuracy of two different versions of Appendix 4 of the R6 method. It is found out that :

i) The results calculated by the new version of Appendix 4 are always conservative. Sometimes, the conservatism may be too large to be acceptable in a practical application.

ii) In a few cases, non-conservative results with a maximum error of 12 % may be generated by the old version of Appendix 4. In other cases, the old method provides less conservative results.

INTRODUCTION

Two different kinds of stresses are defined in the ASME Boiler and Pressure Vessel Code [1], namely primary stresses and secondary stresses. A primary stress is not self-limiting. Primary stresses which exceed the yield strength of the material will result in plastic collapse or in gross distortion. A secondary stress is a self-balancing stress with no resulting net force and moment and hence not able to cause plastic collapse. An example of a primary stress is the stress caused by an internal pressure and an example of a secondary stress is the stress due a temperature gradient.

In recent years, defect tolerance analysis has been applied in Swedish nuclear power plants to obtain suitable in service inspection intervals for different regions of the vessel. In order to facilitate the analysis, effective engineering methods, such as the R6 method [2], are needed. When a structure is subjected to a high thermal load, however, a conservative result is obtained if a linear elastic analysis is performed. In order to reduce the conservatism, an approximate method to treat high secondary stresses is also introduced in Appendix 4 of the R6 method. With the development of the R6 method, different versions of Appendix 4 have been presented [2-4]. It is noted that quite different results can be obtained by the methods described in the different versions of Appendix 4.

The objective of the present analysis is to verify the accuracy of Appendix 4 of the R6 method. For this purpose, two and three dimensional elastic-plastic *J*-integral calculations

have been performed by the finite element method. The results by these calculations are compared to the results by the approximate methods. It should be pointed that only a part of the results are able to presented here. Further results are shown in [5].

THE R6 METHOD

A two parameter failure diagram is introduced in the R6 method, see Fig.1. In Fig. 1, K_r is a measure of the proximity to fracture according to linear elastic fracture mechanics (LEFM), and L_r is a measure of the proximity to plastic collapse. For a particular cracked structure and loading situation, the applied values of K_r and L_r can be calculated. If the point (L_r, K_r) is situated inside the limitations of the failure assessment diagram, the cracked structure is considered to be safe.

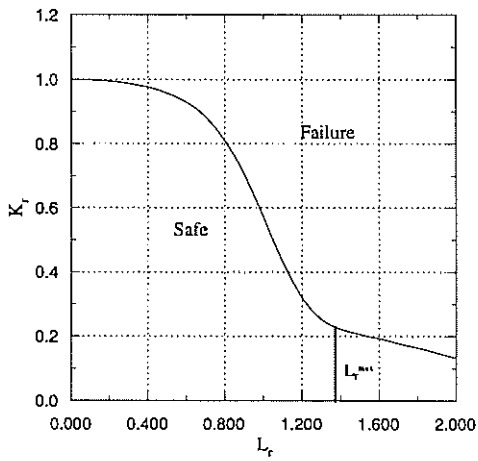

Figure 1. The failure assessment diagram by R6 method .

In the R6 method (option 1), a stress analysis on the uncracked structure is performed. For primary loads, only a linear elastic stress analysis is needed. For secondary loads, both an elastic and an elastic-plastic stress analysis are required. In the following, stresses due to primary loads will be denoted as σ^p, and stresses due to secondary loads as σ^{se} for the elastic analysis and as σ^{sp} for the elastic-plastic analysis. According to Appendix 4, σ^{se} is based on the strain field from the elastic-plastic calculation. For simplicity reason, σ^{se} from a linear elastic calculation is used in Sweden in analysis.

After the determination of stresses, the corresponding linear elastic stress intensity factors are calculated. These results can either obtained by handbook solutions or by finite element calculations. The stress intensity factors due to the above stresses are denoted as K^p, K^{se} and K^{sp} respectively. In addition, an effective crack size can be evaluated as,

$$a_{eff}^{se} = a + \frac{1}{6\pi}\left(\frac{K^{se}}{\sigma_Y}\right)^2, \quad a_{eff}^{sp} = a + \frac{1}{6\pi}\left(\frac{K^{sp}}{\sigma_Y}\right)^2 . \qquad (1)$$

The estimation of the effective stress intensity factor is different for the different versions of Appendix 4. A brief description of them is presented below.

The Old Version of Appendix 4

i) Calculate the stress intensity factors due to σ^{se} and σ^{sp} for the effective crack sizes a_{eff}^{se} and a_{eff}^{sp}. These stress intensity factors are denoted as K_{eff}^{se} and K_{eff}^{sp}, respectively.

ii) Evaluate mean stress intensity factors according to

$$K_1 = \sqrt{K^{se} K^{sp}}, \quad K_2 = \sqrt{K_{eff}^{se} K_{eff}^{sp}}, \tag{2}$$

iii) The stress intensity factor due to the secondary stress is then,

$$K_{old}^{s} = \max\left(K_1, K_2\right), \tag{3}$$

iv) Estimate the parameter ρ which accounts for interaction between primary and secondary loads, see [3].

v) The approximate effective stress intensity factor due to both primary and secondary loads is given by,

$$K_{old} = \frac{K^{p} + K_{old}^{s}}{F\left(L_r\right) - \rho}, \tag{4}$$

where

$$F(L_r) = \left(1 - 0.14 L_r{}^2\right)\left[0.3 + 0.7 \exp(-0.65 L_r{}^6)\right]. \tag{5}$$

The subscript *old* in Eq.(4) indicate the effective stress intensity factor is based on the old version of Appendix 4. For cases when the primary stress is zero,

$$K_{old} = K_{old}^{s}. \tag{6}$$

The New Version of Appendix 4.

i) Calculate the stress intensity factor for the secondary load as,

$$K_{new}^{s} = \left(\frac{a_{eff}^{sp} a_{eff}^{se}}{a^2}\right)^{1/4} \left(K^{sp} K^{se}\right)^{1/2}. \tag{7}$$

Estimate the parameter ρ which takes into account the interaction between primary and secondary loads, see [2]. It should be pointed out that K^s is only used in calculation of parameter ρ. In addition, a negative value of ρ is allowed in the new version of Appendix 4.

ii) The approximate effective stress intensity due to both primary and secondary loads is given by

$$K_{new} = \frac{K^{p} + K^{se}}{F\left(L_r\right) - \rho}, \tag{8}$$

The subscript *new* in Eq. (8) indicates the calculation of the effective stress intensity factor according to the new version of Appendix 4. For cases when the primary stress is zero,

$$K_{new} = K_{new}^{s}. \tag{9}$$

GEOMETRY AND LOADING CONDITION

In the present investigation, a cylinder according to Fig. 2 is considered. The cylinder has an initial uniform temperature of T_0. At time $t = 0$, the temperature at the inner surface of the

cylinder instantaneously drops to zero. The temperature distribution in the cylinder can be described by the following expression,

$$T = T_0\left\{\sum_{n=0}^{\infty}\frac{4}{(2n+1)\pi}\sin\left[\frac{(2n+1)\pi}{2}\left(\frac{x}{w}\right)\exp\left(-\frac{(2n+1)^2\pi^2}{4}\lambda\right)\right]\right\} \quad . \quad (10)$$

In Eq. (10), the non-dimensional parameter λ is defined as

$$\lambda = \frac{d \cdot t}{w^2} \quad , \quad (11)$$

where t is the time and d the thermal diffusivity of the material. The temperature distribution through the thickness of the cylinder at different time instances are shown in Fig. 3. By varying the initial temperature T_0, the effect of different levels of secondary stresses can be studied. The stresses due to the temperature loading are considered to be secondary stresses.

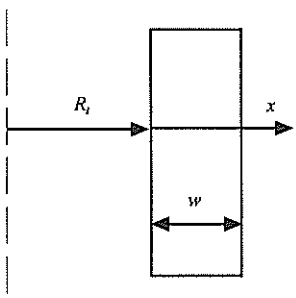

Fig. 2. Studied cylinder.

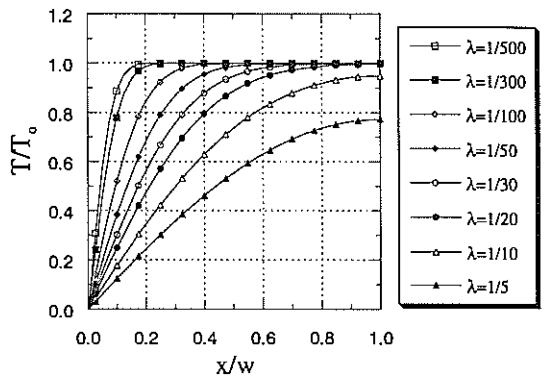

Fig 3. Temperature distribution through the thickness of the cylinder.

FINITE ELEMENT METHOD

Two- and three-dimensional finite element calculations by using the program ABAQUS [6] have been performed. A two dimensional circumferential crack in a cylinder and a three dimensional axial internal surface crack in a cylinder have been studied. 20 node elements with full integration have been used in the three dimensional analysis and 8 node elements in the two dimensional analysis.

In the elastic-plastic analysis, an incremental plastic formulation with small deformation theory has been employed. The 8 different temperature gradients as shown in Fig. 2 have been applied to the model, one after another following the time sequence. The effect of the loading history has also been included in the study. During the investigation, it is observed that the J-integral along the remote integration contours is almost path independent even in case of a non-proportional increase of the loading. Thus the J-integral obtained along a remote path is used to compute the effective stress intensity factor.

The effective stress intensity factors are calculated by J-integral according to,

$$K_{eff} = \sqrt{JE/(1-\nu^2)}, \quad K_{eff} = \sqrt{JE}, \quad , \quad (12)$$

at the deepest point and the free surface of the crack front respectively.

TWO DIMENTIONAL PROBLEM

A complete circumferential crack in a cylinder is considered. The temperature loading shown in Fig. 3 with T_0 = 200 °C has been applied to the cylinder. Three different crack depths are studied, a/w = 0.25, 0.5 and 0.75 respectively. The following material properties are used in the analysis,

Elastic modulus E = 153.86 GPa,
Poisson's ratio ν = 0.3,
Yield stress σ_Y = 196 MPa,
Tangential modulus E_T/E = 0.1 and
Thermal expansion coefficient $\alpha = 2 \cdot 10^{-5}$ 1/°C.

The stress intensity factors at different time points are listed in Tables 1-3 for a/w = 0.25, 0.5 and 0.75, respectively. In these tables, the maximum K-values during the event are marked by bold characters. It can be observed that a good agreement between the maximum values of K_j and K_{old} is obtained except for the case a/w = 0.5 where a slightly non-conservative result (3.6%) is generated by the old version of Appendix 4. Conservative results by the new version of Appendix 4 are generated for all cases. For the case a/w = 0.25, the conservatism is about 36%, see Table 1.

If the temperature gradients at different time points are applied as a set of independent proportional loads, a new set of results can be produced, see Table 4 for a/w = 0.5. It is noted that the results by the new version of Appendix 4 are always conservative. A non-conservative result is obtained by the old version of Appendix 4 (13%). The similar result is observed by Takahashi [7].

Table 1. Stress intensity factors for a/w = 0.25.

λ	K_j (MPa$\sqrt{\text{m}}$)	K_{old} (MPa$\sqrt{\text{m}}$)	K_{new} (MPa$\sqrt{\text{m}}$)
1/500	7.87	9.34	9.60
1/300	10.48	12.31	12.88
1/100	19.18	22.01	24.99
1/50	25.29	28.87	35.27
1/30	28.99	32.32	41.07
1/20	31.30	35.15	**42.91**
1/10	**31.52**	**36.03**	39.53

Table 2. Stress intensity factors for a/w = 0.50.

λ	K_j (MPa$\sqrt{\text{m}}$)	K_{old} (MPa$\sqrt{\text{m}}$)	K_{new} (MPa$\sqrt{\text{m}}$)
1/500	7.02	8.35	8.40
1/300	9.18	13.73	10.86
1/100	15.54	14.07	18.74
1/50	23.60	24.59	26.72
1/30	30.92	30.69	34.68
1/20	35.89	35.05	40.84
1/10	**39.21**	**37.80**	**44.96**

Table 3. Stress intensity factors for a/w = 0.75.

λ	K_j (MPa$\sqrt{\text{m}}$)	K_{old} (MPa$\sqrt{\text{m}}$)	K_{new} (MPa$\sqrt{\text{m}}$)
1/500	6.78	7.670	7.72
1/300	8.93	10.05	10.15
1/100	15.61	16.92	17.41
1/50	20.87	22.26	23.35
1/30	24.89	27.01	28.91
1/20	28.12	30.84	33.61
1/10	**30.76**	**33.85**	**37.46**

Table 4. Stress intensity factors for a/w = 0.50 (proportional load).

λ	K_j (MPa$\sqrt{\text{m}}$)	K_{old} (MPa$\sqrt{\text{m}}$)	K_{new} (MPa$\sqrt{\text{m}}$)
1/500	6.74	8.35	8.40
1/300	9.12	10.73	10.86
1/100	16.40	18.01	18.75
1/50	24.51	24.66	26.82
1/30	32.88	30.89	34.94
1/20	39.08	35.48	41.45
1/10	**44.88**	**39.09**	**46.84**

THREE DIMENSIONAL PROBLEMS

In this section, an internal axial surface crack in a pipe made of an austenitic steel is investigated. It is assumed that the thickness of the pipe w is 25 mm for all cases. Two different piping inner radii are studied, R_i = 250 mm and 1250 mm, respectively. For each pipe, two different crack depths are considered, a = 6.25 mm and 15 mm, respectively. The ratio between the crack length l and the crack depth is 10 (l/a = 10) for all cases. In total, 4 different crack configurations have been studied.

The following material properties are employed in the analysis,

Elastic modulus E = 200 GPa,
Poisson's ratio ν = 0.3,
Yield stress σ_Y = 200 MPa,
Tangential modulus E/E_T= 70 and
Thermal expansion coefficient $\alpha = 19 \cdot 10^{-6}$ 1/°C.

Six different values of T_0 and two different levels of internal pressure are applied to the cylinder. In the analysis, the pressure load is first applied and followed by a temperature load (with a specific T_0), see Eq. (10). One such loading sequence is defined as a loading event. During each event, the maximum stress intensity factor is computed by different methods. The maximum stress intensity factor computed by the different methods may be obtained at different time points and at different crack locations. Normally, the judgement of the risk of fracture is based on the value of the maximum stress intensity factor. The discussions will therefore be focused on the maximum stress intensity factor.

The maximum effective stress intensity factor at the free surface (denoted as the crack tip b) as function of T_0 are presented in Tables 5, 7, 9 and 11. The same results for the deepest point of the crack (denoted as crack tip a) are shown in Tables 6, 8, 10 and 12. The results with nonzero primary stresses are included in Tables 13 and 14.

The parameter C in the tables are defined as,

$$C = \frac{E\alpha}{(1-\nu)\sigma_Y} . \qquad (13)$$

Thus when CT_0 = 6, T_0 = 221 °C which is a reasonable temperature magnitude for a thermal shock in a BWR station.

Table 5.Maximum stress intensity factors at crack tip b for a/w = 0.25, R_i/w = 10 and $pR_i/w\sigma Y = 0$ (L_r = 0).

CT_0	K_J (MPa$\sqrt{\text{m}}$)	K_{old} (MPa$\sqrt{\text{m}}$)	K_{new} (MPa$\sqrt{\text{m}}$)
0	0.00	0.00	0.00
1	12.01	11.91	12.31
2	20.50	21.68	23.30
3	27.36	28.57	31.35
4	31.33	34.59	38.92
5	35.73	39.90	46.99
6	40.83	44.84	55.07

Table 6. Maximum stress intensity factors at crack tip a for a/w = 0.25, R_i/w = 10 and $pR_i/w\sigma Y = 0$ (L_r = 0).

CT_0	K_J (MPa$\sqrt{\text{m}}$)	K_{old} (MPa$\sqrt{\text{m}}$)	K_{new} (MPa$\sqrt{\text{m}}$)
0.0	0.00	0.00	0.00
1.0	12.46	12.32	12.52
2.0	23.48	23.90	25.31
3.0	31.85	32.88	36.52
4.0	37.11	39.33	45.75
5.0	41.22	44.28	53.88
6.0	45.37	48.81	62.18

Table 7.Maximum stress intensity factors at crack tip b for $a/w = 0.60$, $R_i/w = 10$ and $pR_i/w\sigma_Y = 0$ ($L_r = 0$).

CT_0	K_j (MPa$\sqrt{m}$)	K_{old} (MPa$\sqrt{m}$)	K_{new} (MPa$\sqrt{m}$)
0.0	0.00	0.00	0.00
1.0	17.30	17.31	17.92
2.0	31.00	32.46	36.24
3.0	43.30	43.97	52.69
4.0	49.00	53.93	68.88
5.0	54.00	63.06	85.17
6.0	58.30	71.80	101.86

Table 8. Maximum stress intensity factors at crack tip a for $a/w = 0.60$, $R_i/w = 10$ and $pR_i/w\sigma_Y = 0$ ($L_r = 0$).

CT_0	K_j (MPa$\sqrt{m}$)	K_{old} (MPa$\sqrt{m}$)	K_{new} (MPa$\sqrt{m}$)
0.0	0.00	0.00	0.00
1.0	10.640	10.634	10.668
2.0	21.780	20.800	21.124
3.0	31.670	29.939	30.877
4.0	39.930	38.163	40.127
5.0	47.630	45.428	48.776
6.0	53.720	51.364	56.297

Table 9. Maximum stress intensity factors at crack tip a for $a/w = 0.25$, $R_i/w = 50$ and $pR_i/w\sigma_Y = 0$ ($L_r = 0$).

CT_0	K_j (MPa$\sqrt{m}$)	K_{old} (MPa$\sqrt{m}$)	K_{new} (MPa$\sqrt{m}$)
0.0	0.00	0.00	0.00
1.0	11.55	11.34	11.63
2.0	21.00	20.90	21.85
3.0	26.99	27.84	29.18
4.0	30.83	34.00	36.13
5.0	34.86	39.71	43.47
6.0	40.68	44.85	50.82

Table 10. Maximum stress intensity factors at crack tip b for $a/w = 0.25$, $R_i/w = 50$ and $pR_i/w\sigma_Y = 0$ ($L_r = 0$).

CT_0	K_j (MPa$\sqrt{m}$)	K_{old} (MPa$\sqrt{m}$)	K_{new} (MPa$\sqrt{m}$)
0.0	0.00	0.00	0.00
1.0	12.71	13.22	13.47
2.0	23.83	25.43	27.11
3.0	32.13	34.66	38.94
4.0	37.22	41.24	48.68
5.0	41.06	46.35	57.42
6.0	45.59	51.01	66.37

Table 11.Maximum stress intensity factors at crack tip b for $a/w = 0.5$, $R_i/w = 50$ and $pR_i/w\sigma_Y = 0$ ($L_r = 0$).

CT_0	K_j (MPa$\sqrt{m}$)	K_{old} (MPa$\sqrt{m}$)	K_{new} (MPa$\sqrt{m}$)
0.0	0.00	0.00	0.00
1.0	17.00	16.83	17.27
2.0	30.50	32.04	34.74
3.0	43.69	43.99	50.14
4.0	50.62	54.62	65.15
5.0	55.73	64.62	80.15
6.0	60.40	74.00	95.38

Table 12. Maximum stress intensity factors at crack tip a for $a/w = 0.5$, $R_i/w = 50$ and $pR_i/w\sigma_Y = 0$ ($L_r = 0$).

CT_0	K_j (MPa$\sqrt{m}$)	K_{old} (MPa$\sqrt{m}$)	K_{new} (MPa$\sqrt{m}$)
0.0	0.00	0.00	0.00
1.0	11.00	11.01	11.07
2.0	22.96	21.38	21.81
3.0	33.61	30.43	31.66
4.0	43.12	38.48	40.99
5.0	51.38	45.52	49.72
6.0	58.42	51.33	57.54

SUMMARY AND RECOMMENDATIONS

In order to make the discussion easier, the depths of the cracks are divided into three groups, *i.e.* shallow cracks ($0 \le a/t \le 0.45$), median deep cracks ($0.45 \le a/t \le 0.65$) and deep cracks ($0.65 \le a/t \le 1$).

Based on these results, it can be summarised that:

i) For shallow and deep cracks, the old version of Appendix 4 will always provide more accurate and still conservative results when compared to the results by using the new version of Appendix 4.

ii) For median deep cracks, the old version of Appendix 4 may generate non-conservative results (about 125).

iii) For cases when a temperature load combined with a high primary load ($L_r \geq 0.5$), the results by both versions of Appendix 4 are conservative. The conservatism will increase with increasing primary load. In these cases, the elastic-plastic J-integral calculation may be the only method to obtain an accurate result.

iv) The maximum non-conservatism is only about 12% in such a wide range investigation. In comparison with the degree of uncertainty of material data, loads, crack sizes *etc.*, the effect of the non-conservatism in calculation of the stress intensity factor is small. Our opinion is that the old version of Appendix 4 can continually be used as an approximate method to calculate the stress intensity factor for high secondary loads.

Table 13.Maximum stress intensity factors at crack tip a for $a/w = 0.6$, R/w = 10 and $pR_i/w\sigma_Y = 0.2$ ($L_r = 0.39$).

CT_0	K_j (MPa$\sqrt{\text{m}}$)	K_{old} (MPa$\sqrt{\text{m}}$)	K_{new} (MPa$\sqrt{\text{m}}$)
0.0	15.040	14.500	14.500
1.0	25.600	25.210	24.654
2.0	37.940	35.498	35.653
3.0	47.350	44.952	45.364
4.0	55.770	53.912	55.477
5.0	63.060	61.985	64.416
6.0	69.590	68.710	72.284

Table 14. Maximum stress intensity factors at crack tip a for $a/w = 0.6$, R/w = 50 and $pR_i/w\sigma_Y = 0.5$ ($L_r = 0.92$).

CT_0	K_j (MPa$\sqrt{\text{m}}$)	K_{old} (MPa$\sqrt{\text{m}}$)	K_{new} (MPa$\sqrt{\text{m}}$)
0.0	36.05	50.92	50.92
1.0	48.96	69.99	67.80
2.0	64.81	87.60	88.80
3.0	76.38	102.98	105.03
4.0	85.00	116.79	122.20
5.0	93.85	128.84	137.12
6.0	101.95	138.92	151.59

REFERENCES

[1] AMSE Boiler and Pressure Vessel Code, Section III NB, 1995 Edition.

[2] Assessment of the Integrity of Structures Containing Defects, Nuclear Electric, R/H/R6-Revision 3 ,1997.

[3] I. Milne, R.A. Aisworth, A.R. Dowling and A.T. Stewart, "Assessment of the Integrity of Structures Containing Defects". The International Journal of Pressure Vessels and Piping, Vol. 32 pp. 3-104, 1988.

[4] P.J. Budden, "Fracture Assessment of Combined Thermal and Mechanical Load Using Uncracked Body Stress Analysis", CEGB Report RD/B/6158/R89, 1989.

[5] W. Zang, "Assessment of Cracked Components Subjected to High Secondary Stresses", *SAQ/FoU-Report 98/02*, SAQ Control AB, Stockholm, Sweden (1998).

[6] ABAQUS User's and Theory Manuals, version 5.4, Hibbit, Karlsson & Sorensen, Inc. (HKS), USA, 1996

[7] Y. Takahashi, "Study on Simplified Estimation of J-integral under Thermal Loading", SMiRT -12, K. Kussmaul Ed. pp 29-34, 1993.